Cell Reports, Volume *27*

Supplemental Information

HIV-1 Envelope Recognition by Polyreactive and Cross-Reactive Intestinal B Cells

Cyril Planchais, Ayrin Kök, Alexia Kanyavuz, Valérie Lorin, Timothée Bruel, Florence Guivel-Benhassine, Tim Rollenske, Julie Prigent, Thierry Hieu, Thierry Prazuck, Laurent Lefrou, Hedda Wardemann, Olivier Schwartz, Jordan D. Dimitrov, Laurent Hocqueloux, and Hugo Mouquet

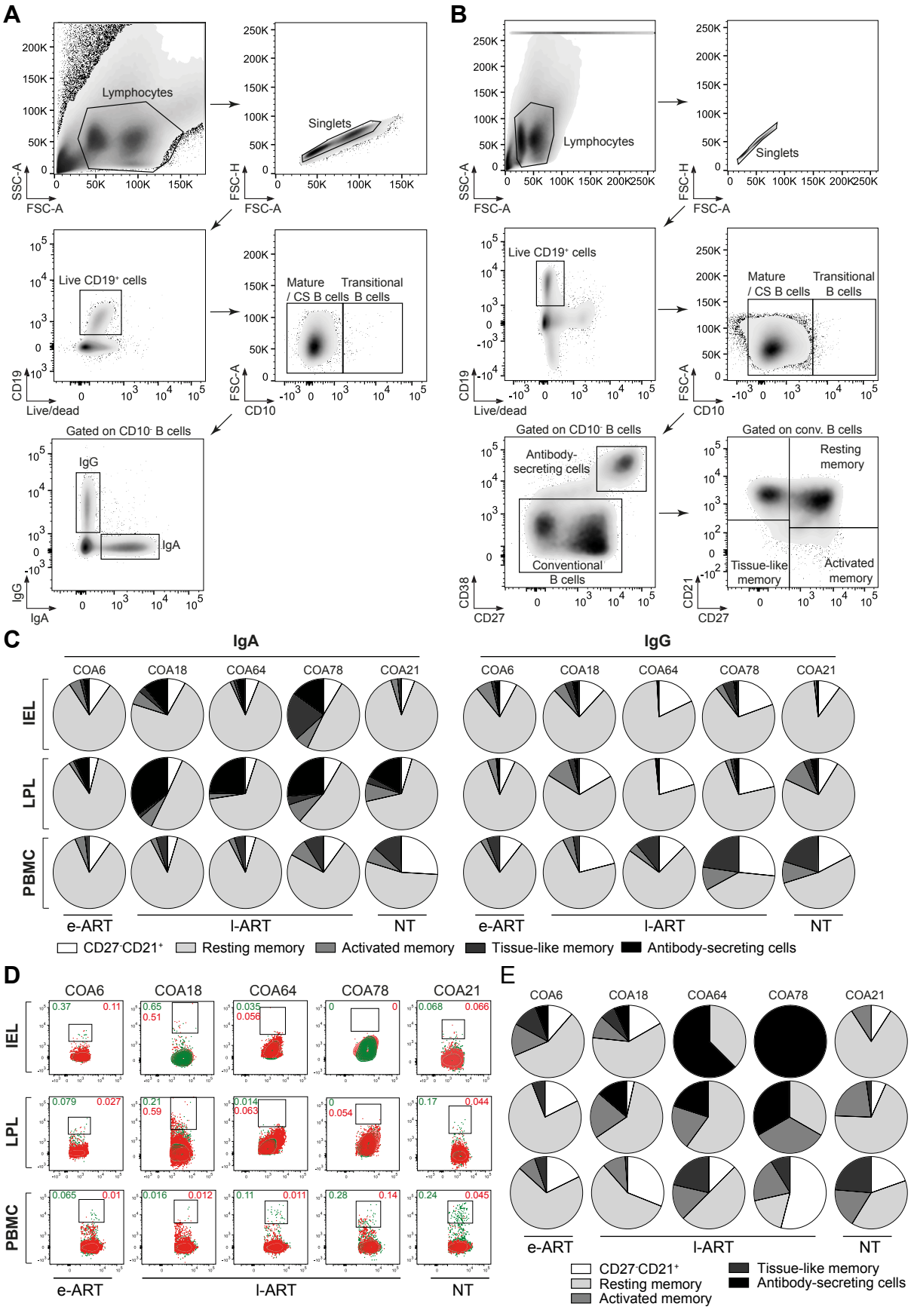

Figure S1. Immunophenotyping of mucosal B-cell subsets from HIV-1-infected individuals (n=5). Related to Figure 1. (**A**) Cytograms show the gating strategy used in flow cytometry analyses to calculate the frequency of the mucosal IgA$^+$ and IgG$^+$ B cells in patients' rectosigmoid biopsies as shown in Figure 1C. (**B**) Cytograms show the gating strategy used in flow cytometry analyses for the immunophenotyping and frequency calculation of the mucosal B-cell subsets in patients' rectosigmoid biopsies as shown in Figure 1D. (**C**) Pie charts comparing the distribution of B-cell subsets in the IEL, LPL and PBMC compartments as determined by flow cytometry for the 5 HIV-1-infected individuals. (**D**) Cytograms show for each donor (n=5), the proportion of single gp140-binding cells among IgG$^+$ and IgA$^+$ B cells. (Bottom) Dot plots comparing the % of IgA$^+$ and IgG$^+$ gp140-reactive B cells. (**E**) Pie charts comparing the distribution of single gp140-binding B cells in the IEL, LPL and PBMC compartments as determined by flow cytometry for the 5 HIV-1-infected individuals.

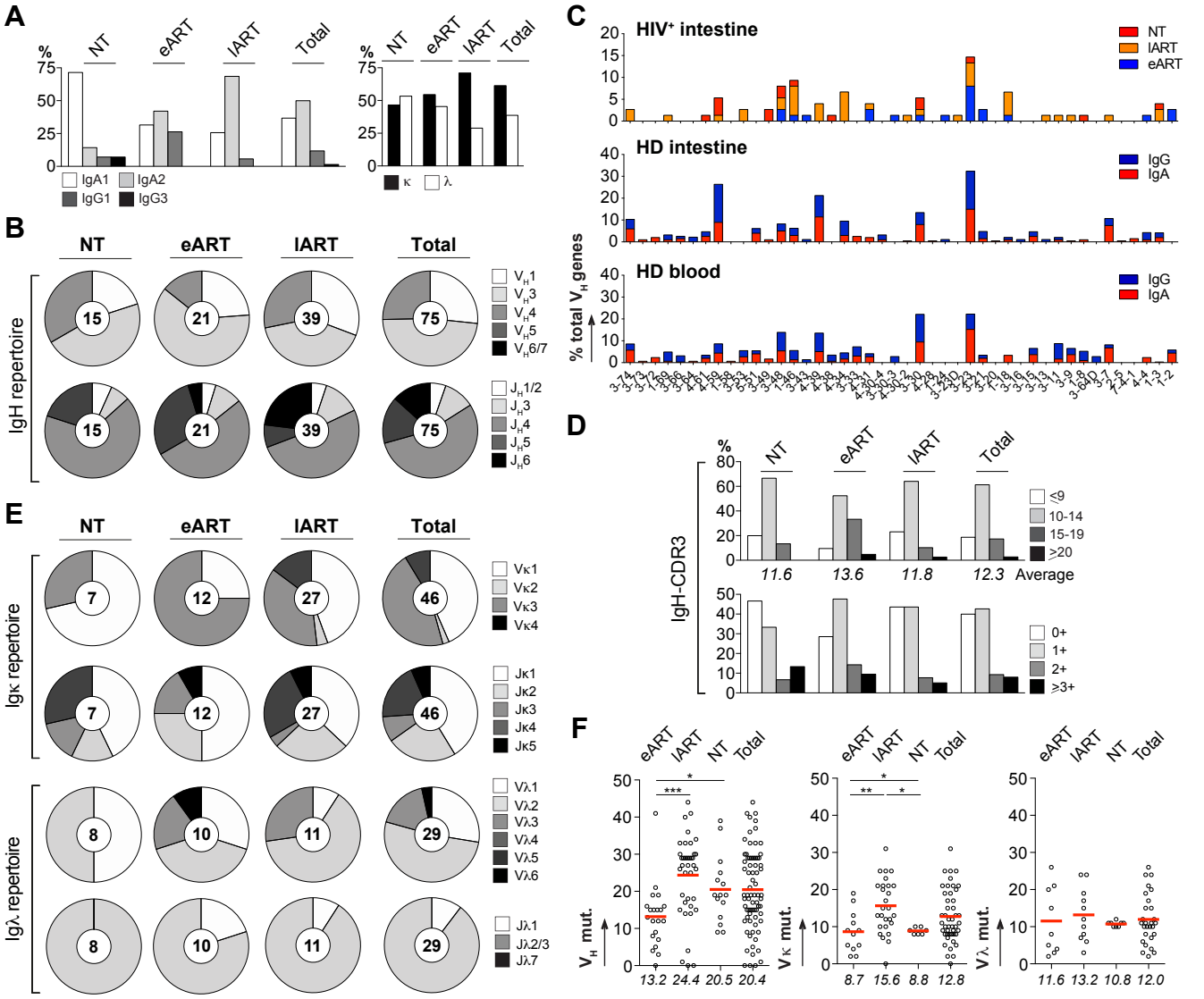

Figure S2. Immunoglobulin gene repertoire of gp140-captured intestinal B cells from HIV-1-infected individuals (n=5). Related to Figure 1. (**A**) Bar graphs show the distribution of IgG/IgA subtypes (Left) and κ- vs λ-Ig chain usage (Right) in gp140-captured mucosal B cells. (**B**) IgH and IgL gene usages. Pie charts show the distribution of V_H / J_H gene usage in gp140-captured mucosal B cells. The number of antibody sequences analyzed is indicated in the center of each pie chart. (**C**) Bar graph comparing the distribution of single immunoglobulin V_H genes expressed by intestinal B cells of HIV-1-infected donors (combining NT, eART and lART donors), total intestinal IgG^+/IgA^+ plasmablasts (Benckert et al., 2011) and blood IgG^+/IgA^+ memory B cells (Prigent et al., 2016) from healthy individuals. (**D**) Bar graphs show the distribution of CDR_H3 lengths and positive charge numbers in gp140-captured mucosal B cells. The average of CDR_H3 lengths is indicated above each histogram. (**E**) Pie charts show the distribution of $V_κ$ / $J_κ$ and $V_λ$ / $J_λ$ gene usage in gp140-captured mucosal B cells. The number of antibody sequences analyzed is indicated in the center of each pie chart. (**F**) Dot plots show the number of mutations in V_H, Vκ and Vλ genes gp140-captured mucosal B cells. The average number of mutations (mut.) is indicated below each dot plot. Numbers of mutations were compared across groups of antibodies using unpaired student t-test with Welch's correction. *, p<0.05; **, p<0.01; ***, p<0.001.

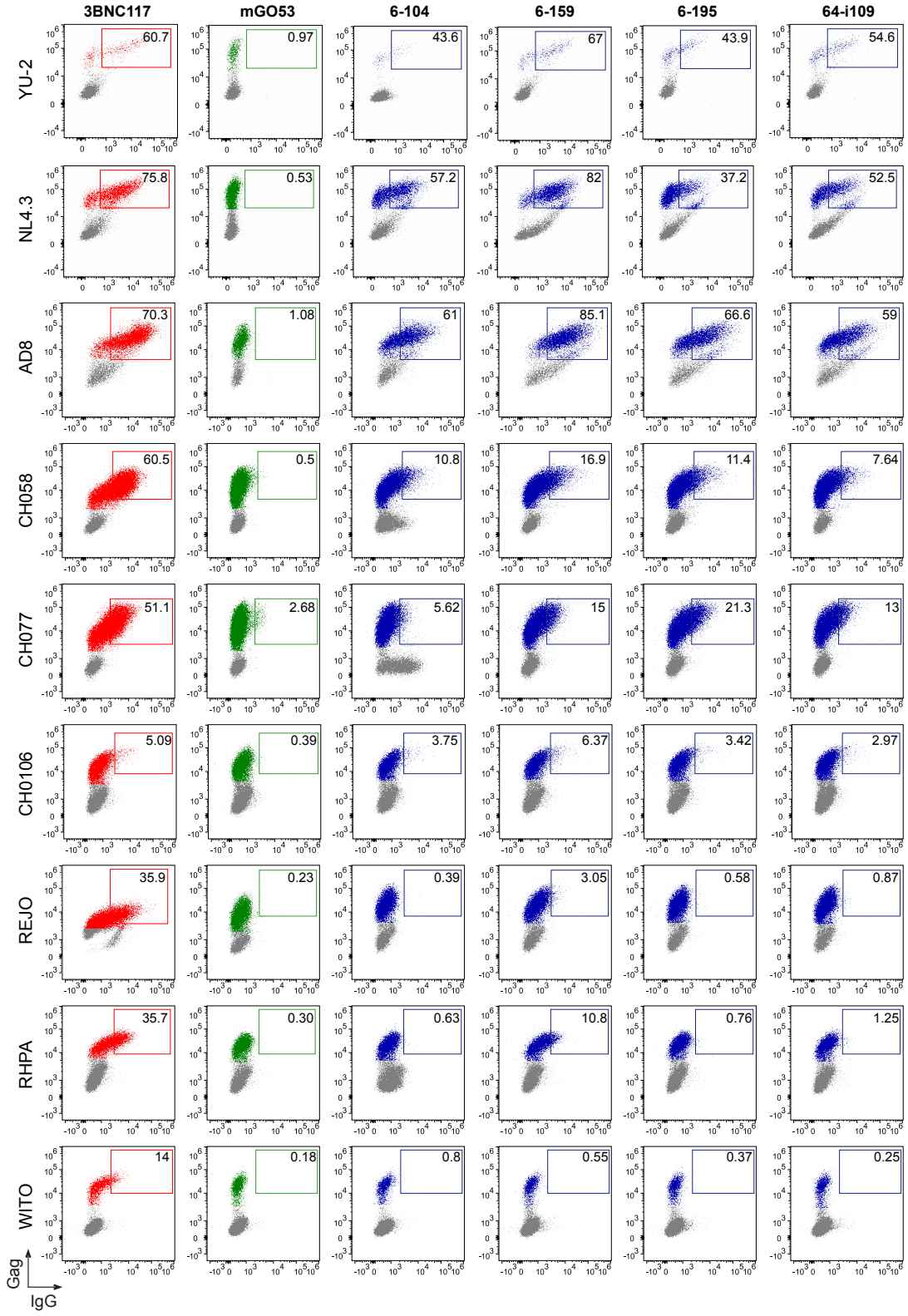

Figure S3. Binding of mucosal gp160-specific antibodies to HIV-1-infected cells. Related to Figure 2. Representative cytograms show the binding of mucosal anti-gp140 and control IgG antibodies to Gag^+ target cells infected with the selected viruses. 3BNC117 (Scheid et al., 2011) and mGO53 (Wardemann et al., 2003) are positive and negative control, respectively. The % of Gag^+ cells bound by antibody is indicated in the right-end upper corner of the gate.

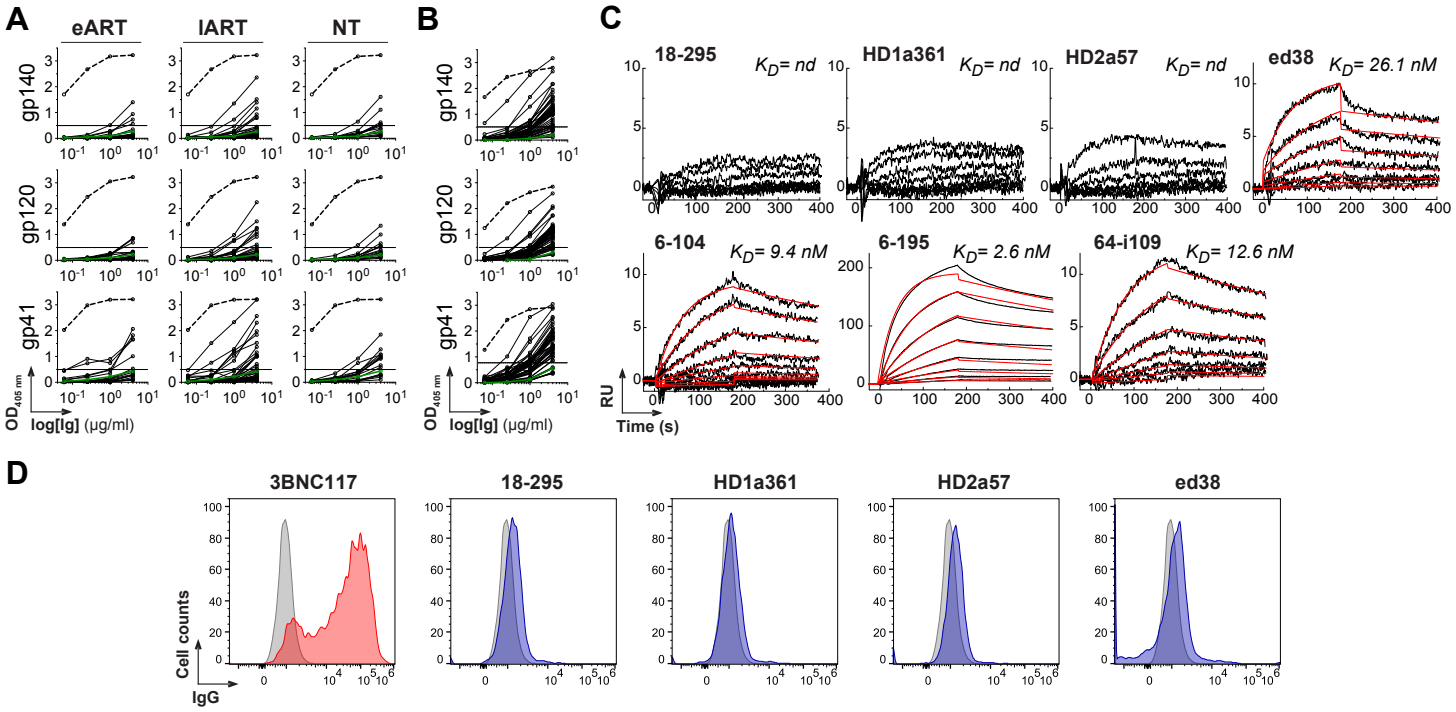

Figure S4. Polyreactive binding to HIV-1 envelope proteins. Related to Figure 3. (**A**) ELISA graphs show the reactivity of intestinal IgG mAbs from mucosal antibodies isolated from HIV-1-infected individuals (n=72) against clade B trimeric gp140, gp120 and gp41 proteins in the experimental conditions to measure polyreactivity (see Experimental Procedures). mGO53 (Wardemann et al., 2003) (green lines) and ED38 (Meffre et al., 2004) (dotted lines) are negative and positive control antibody, respectively. Horizontal lines show cut-off $OD_{405\ nm}$ for positive reactivity. Mean values from two independent experiments are shown. (**B**) Same as for (A) but for polyreactive intestinal IgG mAbs from healthy individuals (n=41) (Benckert et al., 2011). (**C**) SPR sensorgrams comparing the binding of selected antibodies to trimeric ZM96 gp140 glycoproteins. The y axis shows the response units (RU) obtained at a given time (s, seconds) indicated on the x axis. (**D**) Flow cytometry histograms show the binding of selected IgGs to YU-2-infected cells (colored) compared to non-infected target cells (grey). 3BNC117 (Scheid et al., 2011) is the positive control.

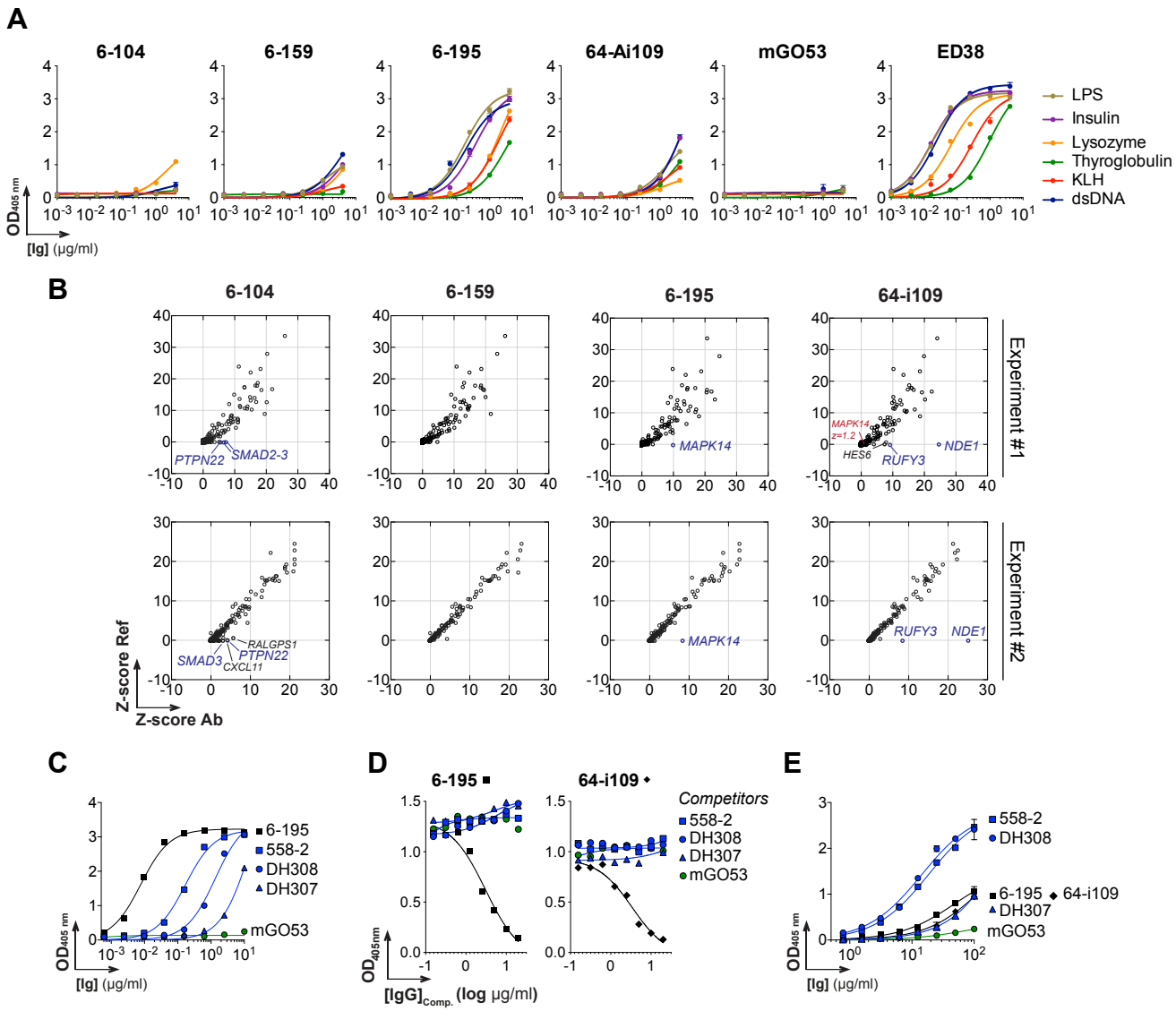

Figure S5. Poly- and cross-reactivity of mucosal HIV-1 antibodies. Related to Figure 4. (**A**) Representative ELISA graphs show the reactivity of mucosal HIV-1 antibodies against dsDNA, ssDNA, insulin, keyhole limpet hemocyanin (KLH), thyroglobulin and lysozyme. mGO53 (Wardemann et al., 2003) and ED38 (Meffre et al., 2004) are negative and positive control antibody, respectively. Mean of duplicate values are shown. (**B**) Protein microarray plots show the reactivity profile of mucosal anti-gp140 antibodies against human proteins obtained in two independent experiments. For each protein spot, Z-scores given by the reference (Ref: mGO53) and test antibody are depicted on the y and x axis, respectively. Blue dots correspond to the immunoreactive proteins identified in both experiments. RALGPS1, Ral GEF with PH domain and SH3 binding motif 1. (**C**) ELISA graphs show the reactivity of previoulsy cloned mucosal anti-gp41 cluster I antibodies (Liao et al., 2011; Trama et al., 2014) to MN gp41. mGO53 and 6-195 are negative and positive control antibody, respectively. Mean of duplicate values are shown. (**D**) ELISA graphs show the binding of biotinylated 6-195 and 64-i109 antibodies to gp41 in the presence of mucosal anti-gp41 cluster I antibodies (Liao et al., 2011; Trama et al., 2014). Mean of duplicate values are shown. (**E**) Representative ELISA graphs show the reactivity of the selected antibodies to E. coli RNA polymerase subunit a. mGO53 is the negative control. Error bars indicate the SEM of duplicate values.

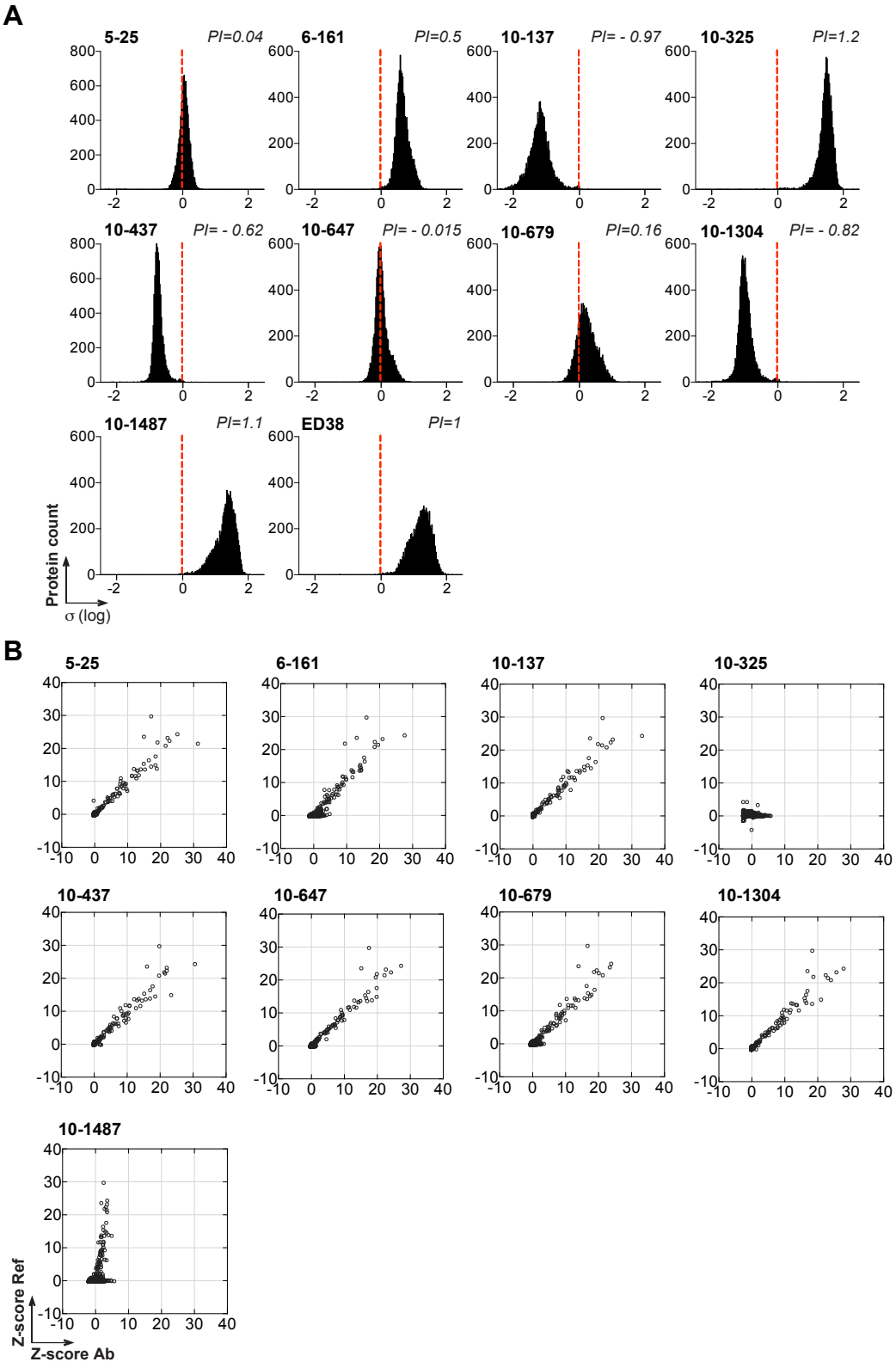

Figure S6. Poly- and cross-reactivity of blood HIV-1 gp41 antibodies. Related to Figure 5. (**A**) Frequency histograms show the $\log_{10}$ protein displacement (σ) of the MFI signals for the selected antibodies compared to non-HIV-1 control antibody mGO53 (Wardemann et al., 2003). The polyreactivity index (PI) corresponds to the Gaussian mean of all array protein displacements. (**B**) Protein microarray plots show the reactivity profile of mucosal anti-gp140 antibodies against human proteins. For each protein spot, Z-scores given by the reference (Ref: mGO53) and test antibody are depicted on the y and x axis, respectively.

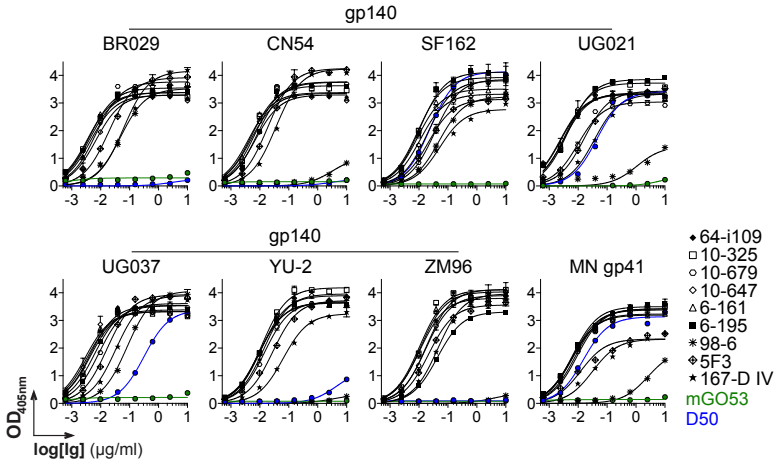

Figure S7. Reactivity of anti-gp41^{HR2} antibodies to various HIV-1 Env proteins. Related to Figure 6. ELISA graphs show the reactivity of human anti-gp41^{HR2} (Gorny et al., 1989; Xu et al., 1991; Buchacher et al., 1994; Scheid et al., 2009; Mouquet et al., 2011), and murine D50 (Earl et al., 1997) antibodies to the selected trimeric gp140 and gp41 proteins. mGO53 (Wardemann et al., 2003) is the negative control. Error bars indicate the SEM of duplicate values.